KU LEUVEN

UNIVERSITY OF TURKU

SWATNet

Planetary, solar and heliospheric Radio Emissions X

11-13 Jun 2025 Marseille (France)

Modelling Gyrosynchrotron Emission from Energetic Electrons in CME Flux Ropes

E. Husidic[1,2] , N. Wijsen[1], I. C. Jebaraj[2], A. Vourlidas[3], L. Linan[1], R. Vainio[2], S. Poedts[1,4]

[1]Department of Mathematics, KU Leuven, Leuven, Belgium
[2]Department of Physics and Astronomy, University of Turku, Turku, Finland
[3]The John Hopkins University Applied Physics Laboratory, Maryland, USA
[4]Institute of Physics, University of Marie Curie-Sklodowska, Lublin, Poland

PREX Conference, Marseille, France, 11 – 13 June 2025

SWATNet has received funding from the European Union’s Horizon 2020 research and innovation programme under the Marie Sklodowska-Curie Innovative Training Networks Grant Agreement No 955620.

Outline

- Introduction
- Modelling Framework
- Simulation Results
- Summary and Outlook

Introduction

Type IV Radio Bursts

- The solar atmosphere is a rich source of radio emission, especially during/after solar flares and CMEs
- Type IV bursts: broadband continua, often containing bursty features, during/after CMEs and flares
- Complex interplay of processes
  - **Coherent** vs. **incoherent** emission (Melrose 2017)
  - **Spontaneous** vs. **stimulated** emission (Papadopoulos & Freund 1979)
  - **Thermal** vs. **nonthermal** processes (Pick & Vilmer 2008)

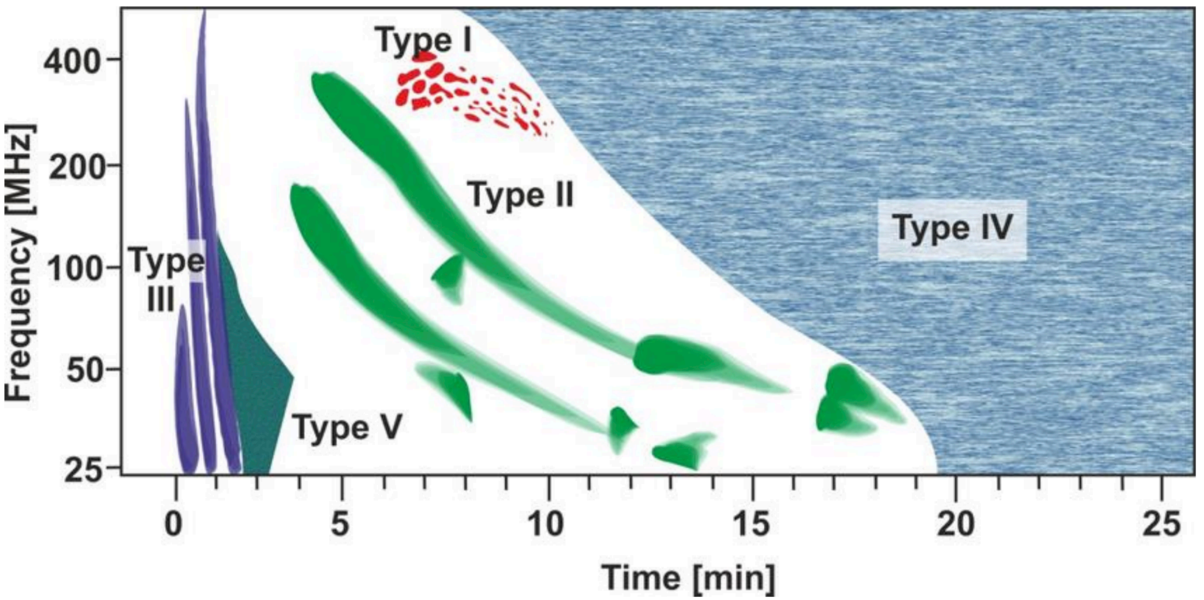

Fig: Different types of radio bursts (Shamsuddin+2023)

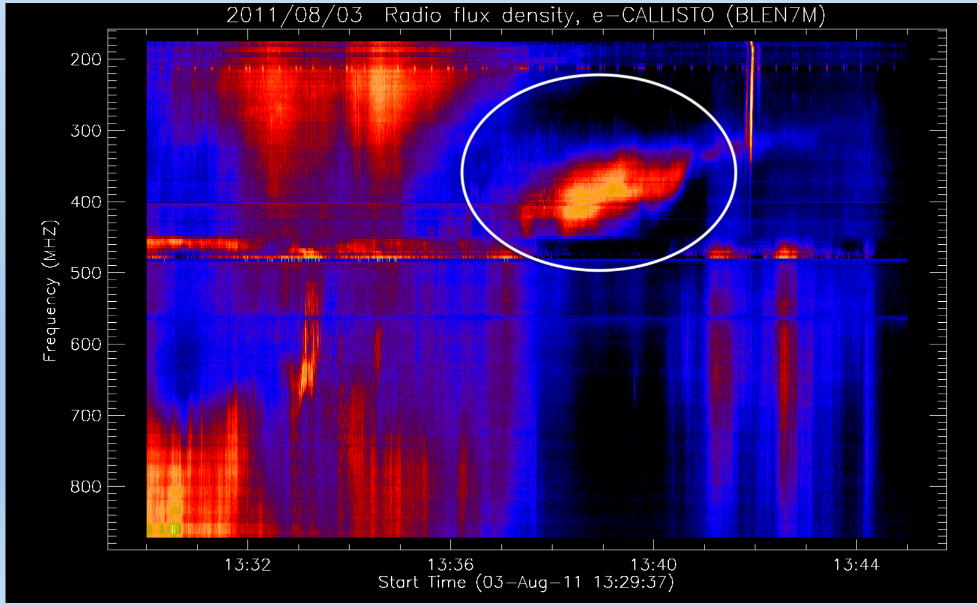

Fig: Dynamic radio spectrum of a type IV burst

Challenges in Interpreting Type IV Bursts

- Disentangling emission mechanisms (Morosan+2019)
- **Diagnosing** CME magnetic fields from radio spectra (Mondal+2020)
- **Stationary** (IVs) vs. **moving** (IVm) type IV sources (Morosan+2021)
  - ➢ Spectral drift ≠ spatial drift – imaging reveals spatial motion **even without** frequency drift
- IVm/IVs classification is blurred
  - ➢ Gyrosynchrotron (GS) sources naturally show spatial drift (CME motion); apparent stationarity can result from coherent emission processes

Morosan+2021

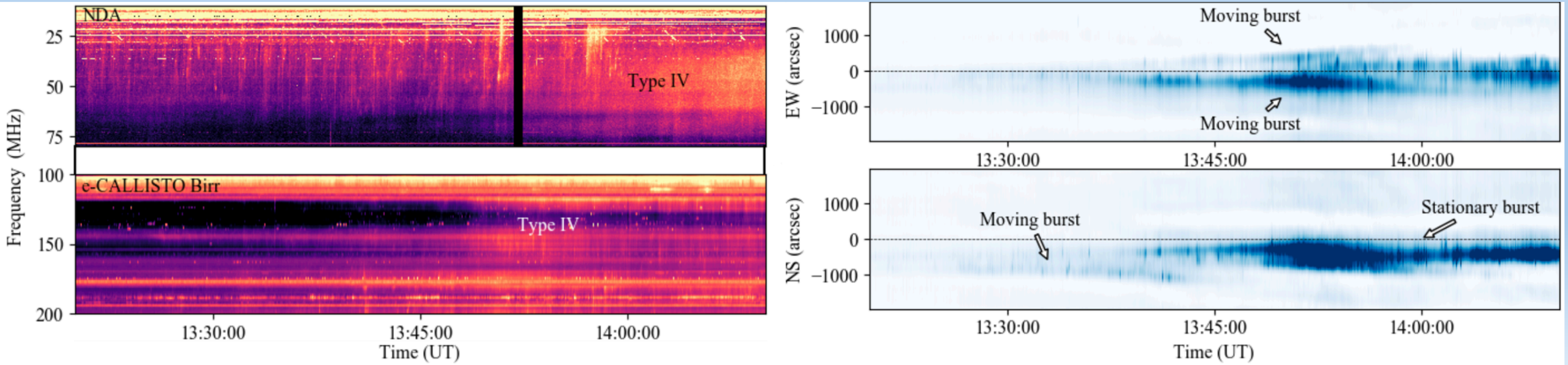

Aims and Coupled Modelling Approach

Aims:

- Simulate **GS emission** from energetic electrons trapped in erupting CME flux ropes

- Move **beyond idealised assumptions** about corona and electron distributions

- Investigate **how synthetic type IV spectra are shaped** by:

  - Variations in the electron energy distributions
  - CME properties and dynamics
  - Observer perspective

Aims and Coupled Modelling Approach

Aims:

- Simulate **GS emission** from energetic electrons trapped in erupting CME flux ropes

- Move **beyond idealised assumptions** about corona and electron distributions

- Investigate **how synthetic type IV spectra are shaped** by:

  - Variations in the electron energy distributions
  - CME properties and dynamics
  - Observer perspective

Coupled Modelling Approach:

- Modular simulation chain linking:

  - **Coronal plasma dynamics** including CMEs (MHD model)
  - **Energetic electron transport** (particle transport code)
  - **Radio emission synthesis** (gyrosynchrotron code)

Modelling Framework

Modelling Framework

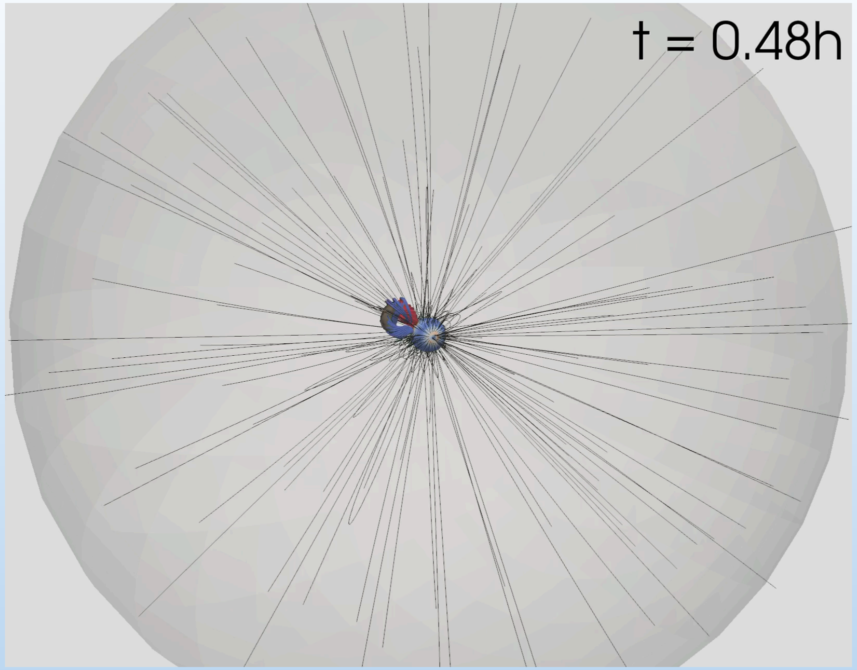

Husidic+2024

COCONUT - COolfluiD COroNal UnsTructured

- 3D **ideal MHD** model of the corona (Perri+2023)
- CME: unstable Titov-Démoulin **flux rope** (Linan+2023)

PARADISE (PArticle Radiation Asset Directed at Interplanetary Space Exploration)

- Evolves energetic particles through dynamic MHD fields
- Solves **focused transport equation** stochastically (Wijsen 2020)

Ultimate Fast Gyrosynchrotron Codes (UFGSCs)

- Calculate **GS emission** and **absorption**
- Use **fast, accurate numerical approximations** (Fleishman & Kuznetsov 2010)
- Allow for **arbitrary electron distributions** (Kuznetsov & Fleishman 2021)

Simulation Setup

- **Two eruption strengths** in the CME simulation:
  - ➢ $\zeta = 30 \rightarrow B_0 \approx 5.8$ G; $v_0 \approx 940$ km/s
  - ➢ $\zeta = 70 \rightarrow B_0 \approx 10.6$ G; $v_0 \approx 1300$ km/s

- **Two power-law indices** for electron injections: $\delta = 2$ and $\delta = 3$ (10 keV to 10 MeV)

- **Three observer perspectives** (“**helio** view”, “**edge-on** view”, ”**face-on** view”) with defined **viewing fields**

- **Calculate GS emission** along **lines of sight** and integrate over observer’s field of view

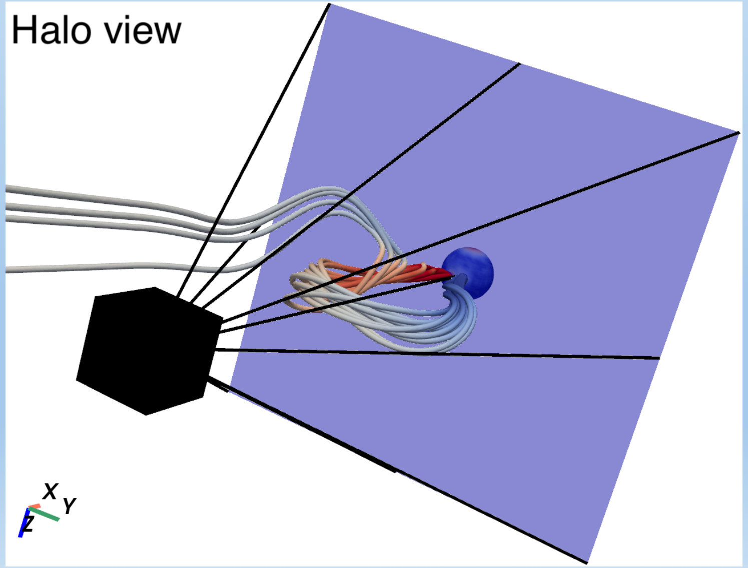

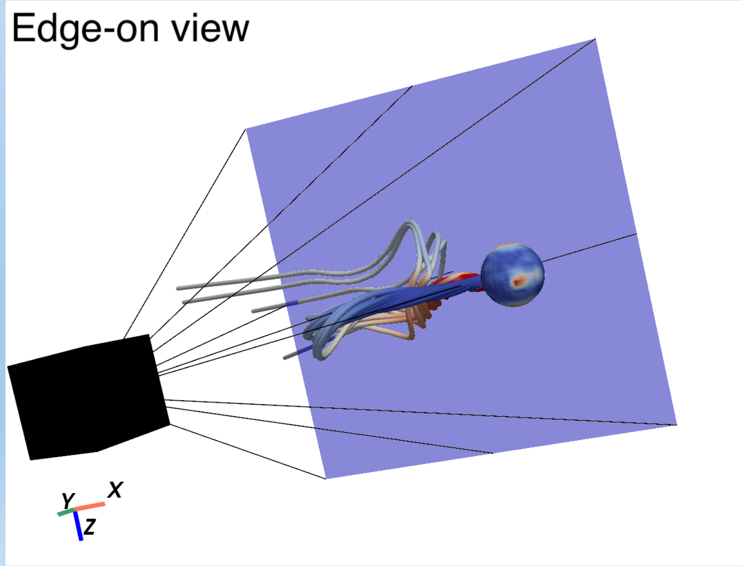

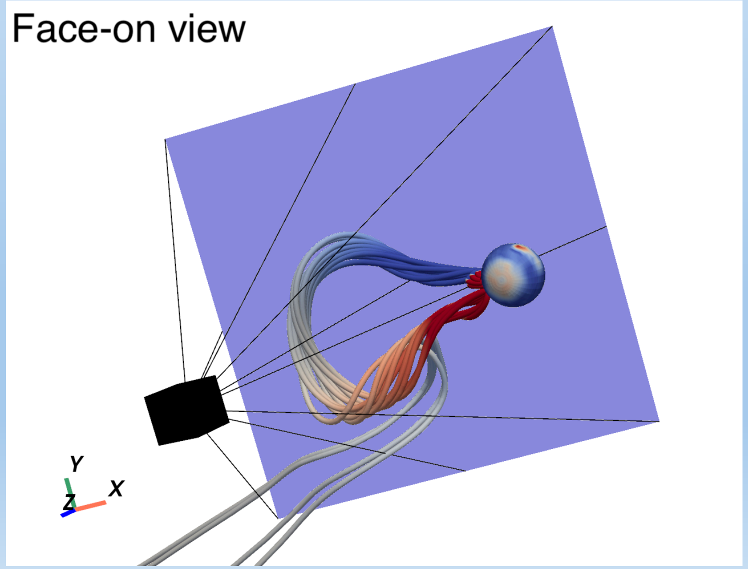

Observer is inside the corona (r < 0.1 au = 21.5 solar radii)

Husidic et al. (submitted)

Simulation Results

CME Case ζ = 30

Peak intensity ratios across δ-values:

View	$I_{\delta=2}/I_{\delta=3}$
halo	1100
edge-on	564
face-on	560

Peak intensity ratios across views:

δ	$I_{\mathrm{edge-on}}/I_{\mathrm{halo}}$	$I_{\mathrm{face-on}}/I_{\mathrm{halo}}$
2	13.1	22.5
3	25.5	44.1

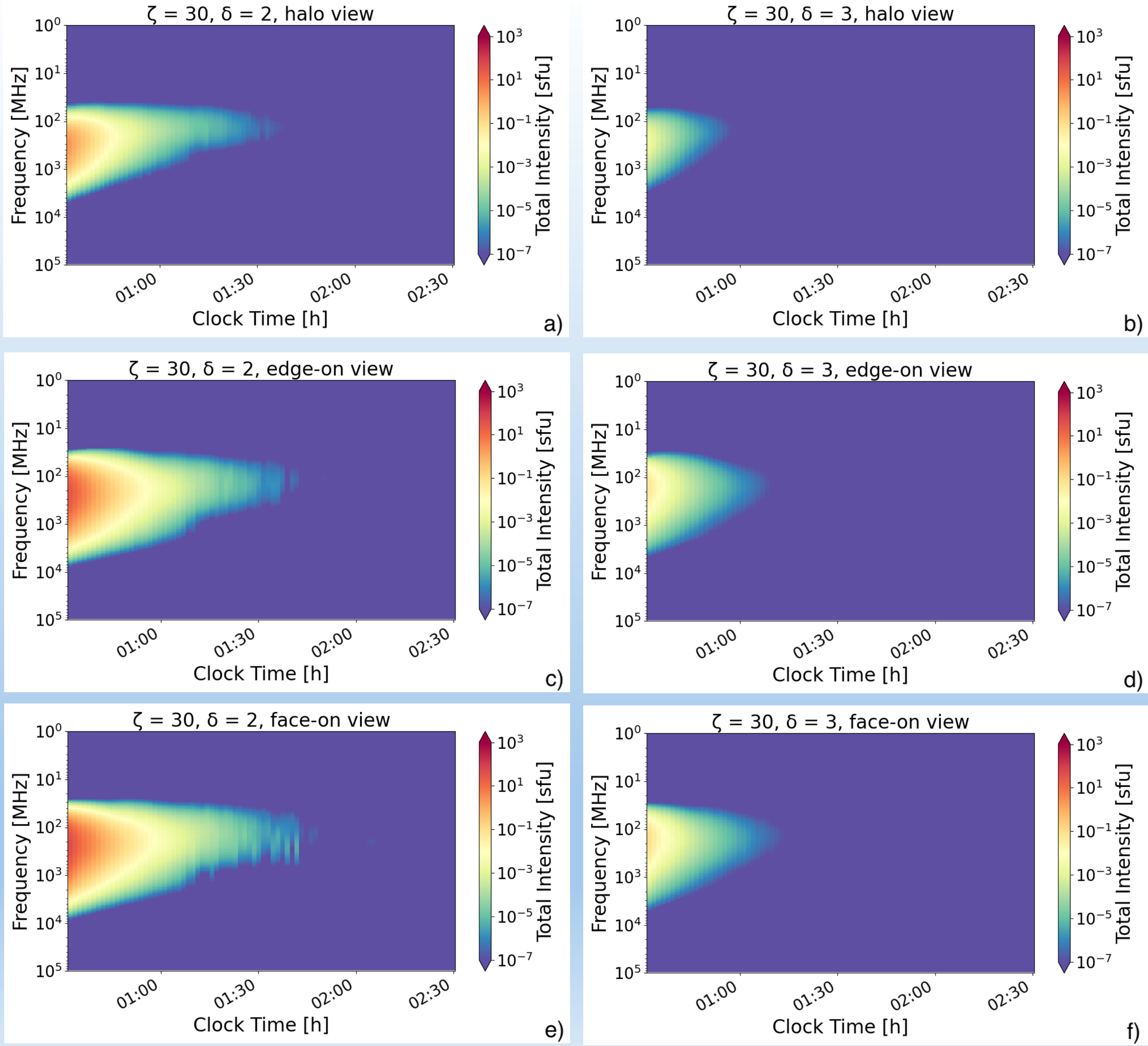

Husidic et al. (submitted)

CME Case ζ = 30

- **Flatter spectrum** (δ = 2) → more high-energy electrons
  → **stronger** and **longer** lasting GS emission

- **GS intensity** depends on **B-field strength** and **observer geometry**

  - ➢ **Helio view**: weakest emission (aligned fields, thinner region)
  - ➢ **Edge-on view**: stronger emission (thicker flux rope cross section, stronger fields)
  - ➢ **Face-on view**: strongest emission (optimal viewing angle + large region)

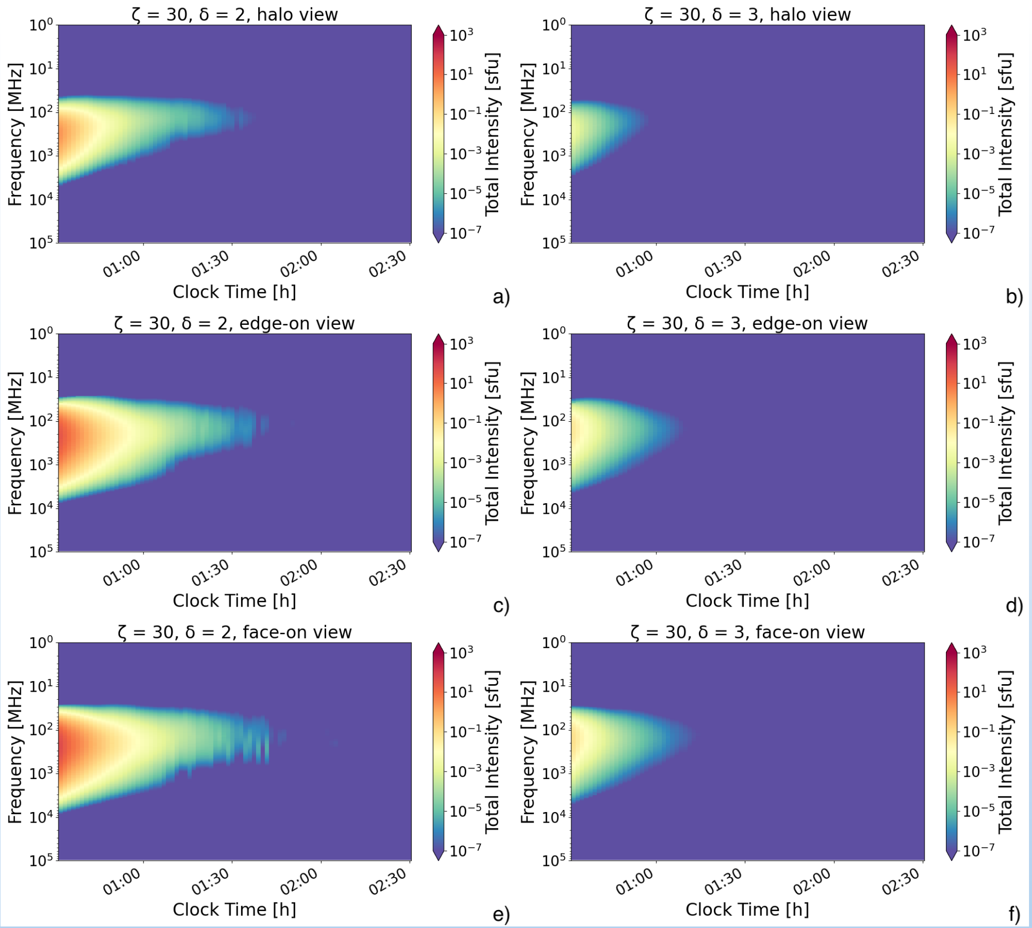

Husidic et al. (submitted)

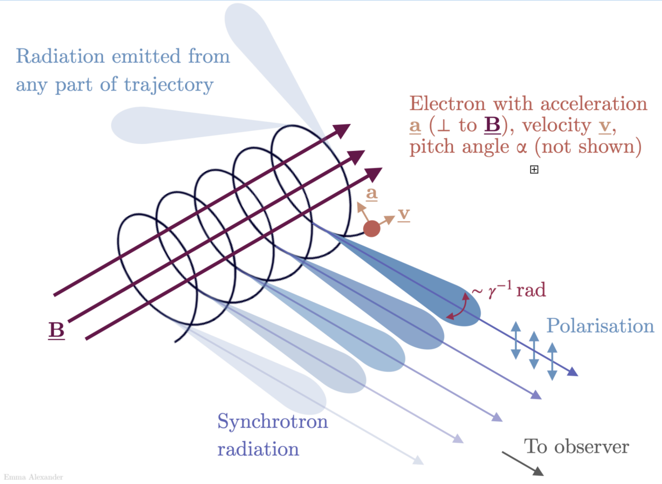

Credit: Emma Alexander, under CC BY 4.0.

CME Case ζ = 70

Peak intensity ratios across δ-values:

View	$I_{\delta=2}/I_{\delta=3}$
halo	620
edge-on	310
face-on	208

Peak intensity ratios across views:

δ	$I_{\text{edge-on}}/I_{\text{halo}}$	$I_{\text{face-on}}/I_{\text{halo}}$
2	7.2	12.8
3	14.3	38.1

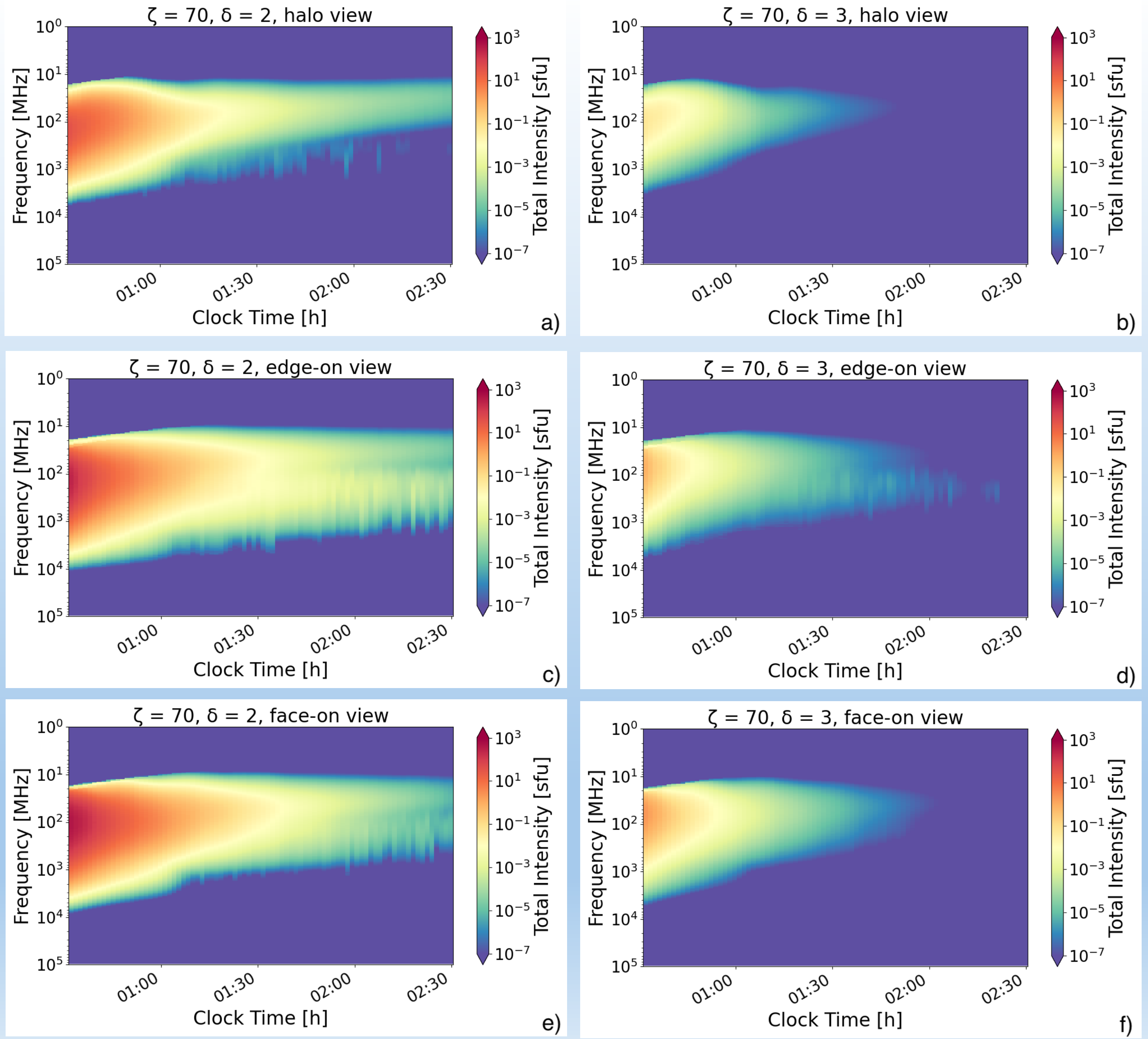

Husidic et al. (submitted)

CME Case ζ = 70

- **Similar trends** as ζ = 30 cases

- **Secondary emission lane** detected at higher frequencies (edge-on/face-on views)

    - ➢ Localised GS enhancements from stronger B-fields

$$P_{\mathrm{syn}} \approx \frac{4}{3}\,\sigma_{\mathrm{T}}\,c\,\gamma^2\,\beta^2\,U_B\,\sin^2\alpha$$

σ_{T}: Thomson scattering cross-section
$\beta = v/c$
$U_{\mathrm{B}} = B^2/(8\,\pi)$ magnetic energy density
α: pitch-angle

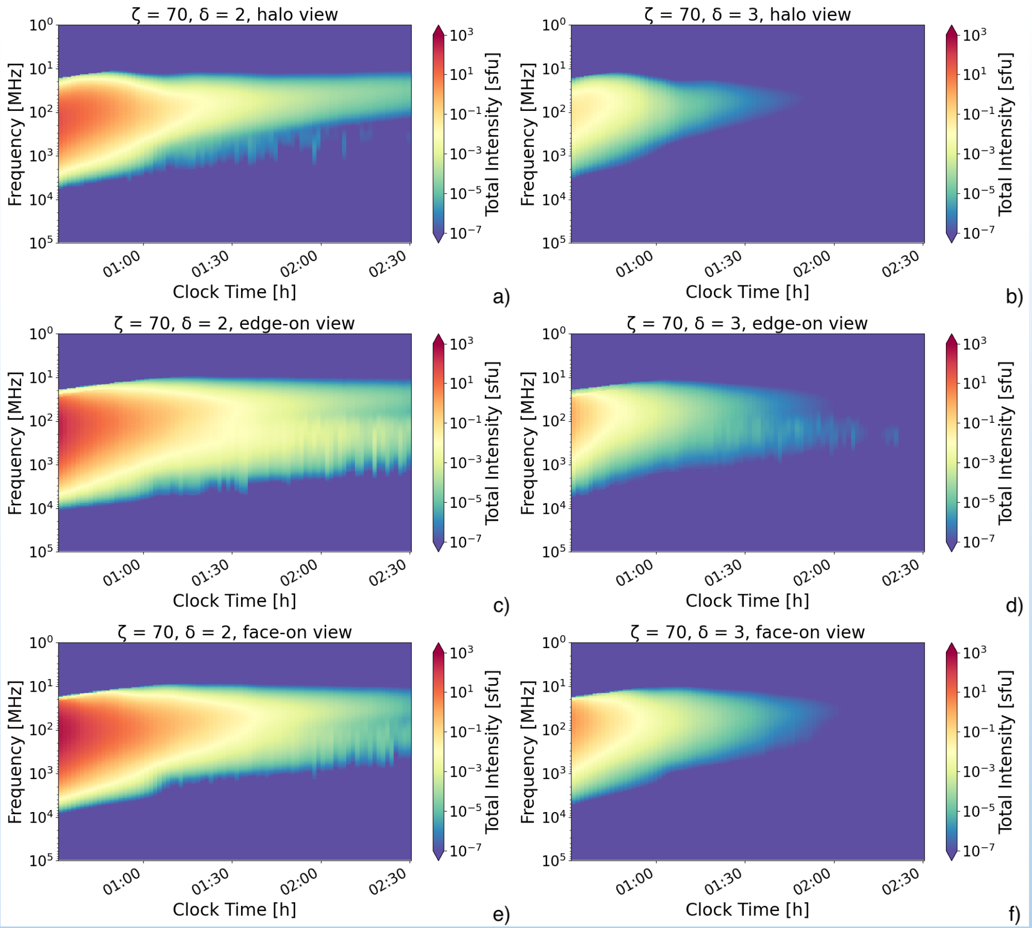

Husidic et al. (submitted)

Intensity Ratios across CME Cases

(3) Intensity ratios across CME cases

δ	View	$I_{\zeta=70}/I_{\zeta=30}$
2	halo	16.2
	edge-on	8.9
	face-on	9.2
3	halo	28.6
	edge-on	16.1
	face-on	24.7

Husidic et al. (submitted)

ζ = 70 CME yields stronger GS emission across vantage points

Stronger magnetic fields → increased synchrotron power

Stronger field gradients enhance electron trapping and GS emission

$$P_{\mathrm{syn}} \approx \frac{4}{3}\sigma_{\mathrm{T}}\, c\, \gamma^2 \beta^2\, U_B\, \sin^2\alpha$$

σ_{T}: Thomson scattering cross-section
$\beta = v/c$
$U_{\mathrm{B}} = B^2/(8\,\pi)$ magnetic energy density
α: pitch-angle

Summary and Outlook

Summary and Outlook

- **Coupled Numerical Models**
  - **COCONUT** : 3D MHD coronal model
  - **PARADISE** : Energetic particle transport simulations
  - **UFGSCs** : Fast GS emission computations

- **Modelling GS Emission in the Corona**
  - Type IV spectra are shaped by **electron index**, **CME properties**, and **observer geometry**
  - Strongest GS emission originates from **CME legs**
  - Results support **GS** as a **key contributor** of type IV bursts
  - **Coherent** plasma processes **cannot be excluded**

- **Outlook**
  - Future parametric studies will explore how **CME B-fields** shape GS signatures
  - Aim to address the **stationary vs. moving type IV conundrum**
  - Use **PSP in situ data** (radio waves, particles) to **constrain model** and link to **observed events**

Backup Slides

Peak Intensity Frequency Drift

- All obtained spectra exhibit similar structure, featuring a high-intensity centre surrounded by weaker emission, with the peak drifting towards lower frequencies over time
- Compare to characteristic synchrotron peak frequency (Ginzburg 1979)

$$\nu_{\mathrm{peak}}(t) = \frac{3}{4\pi}\frac{e\,B(t)}{m_{\mathrm{e}}\,c}\,\gamma^2 = \frac{3}{4\pi}\,\nu_{\mathrm{g}}(t)\,\gamma^2$$

- Both CME expansion and adiabatic cooling contribute to observed downward drift in the simulation results

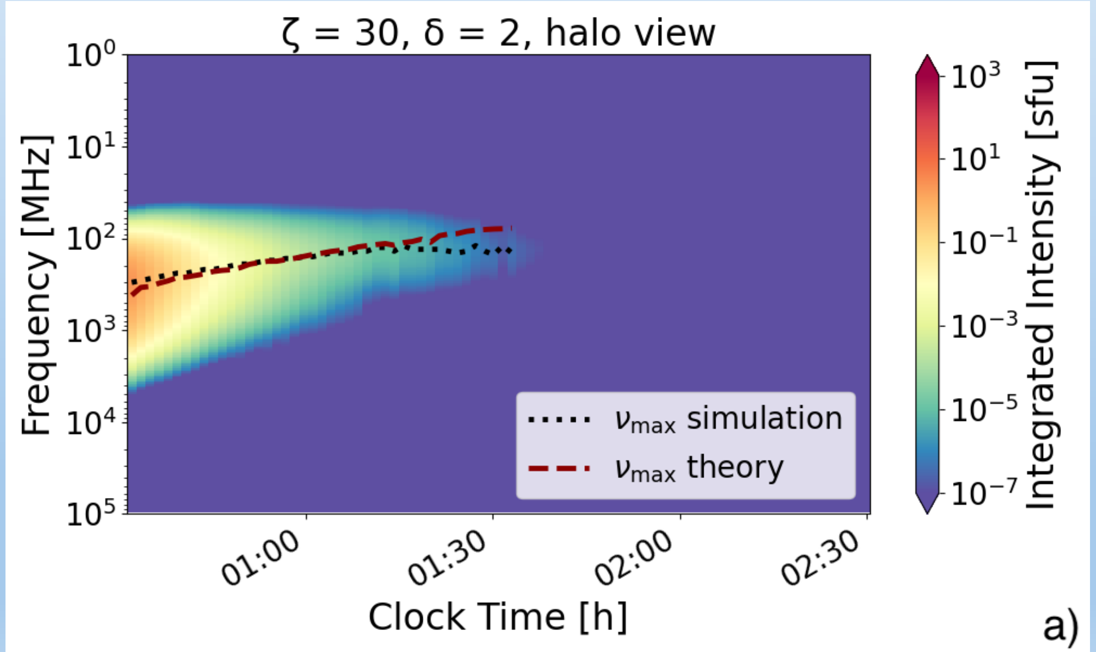

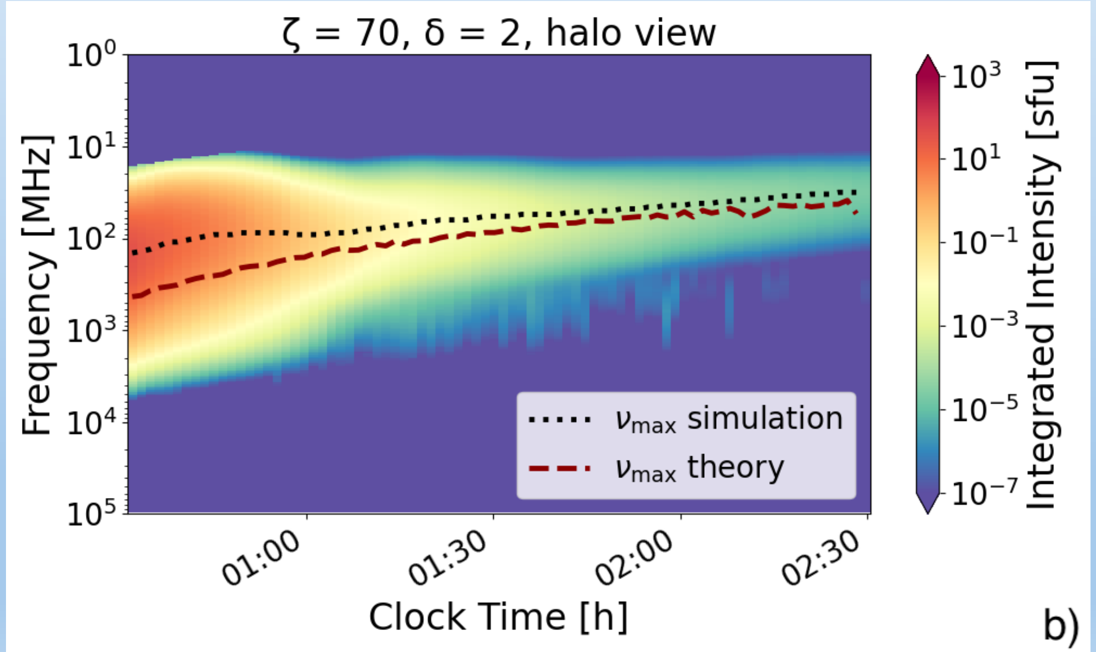

Fig: Peak intensity frequency drifts from simulation and theory (Husidic et al., submitted)

PARADISE Distribution Scaling

- Output: differential intensity $$j(\mathbf{x}, \mathbf{p}, t) = p^2 f(\mathbf{x}, \mathbf{p}, t)$$
- Provide electron distributions as $f_{i,j} = f(E_i, \mu_j)$ to the UFGSCs, where energies are logarithmically spaced
- PARADISE distribution scaled to match a (relativistic regularised) Kappa distribution (rRKD, κ = 8) at 10 keV at injection location and injection time
- To avoid exact zeros in the electron distribution, an rRKD background is added
- Background ensures:
  - Physical units of *f*
  - Avoiding excessively steep gradients in *f* that could otherwise provide conditions for maser instability to grow
- Background contribution to GS emission is negligible (< 0.01 % at peak intensity)

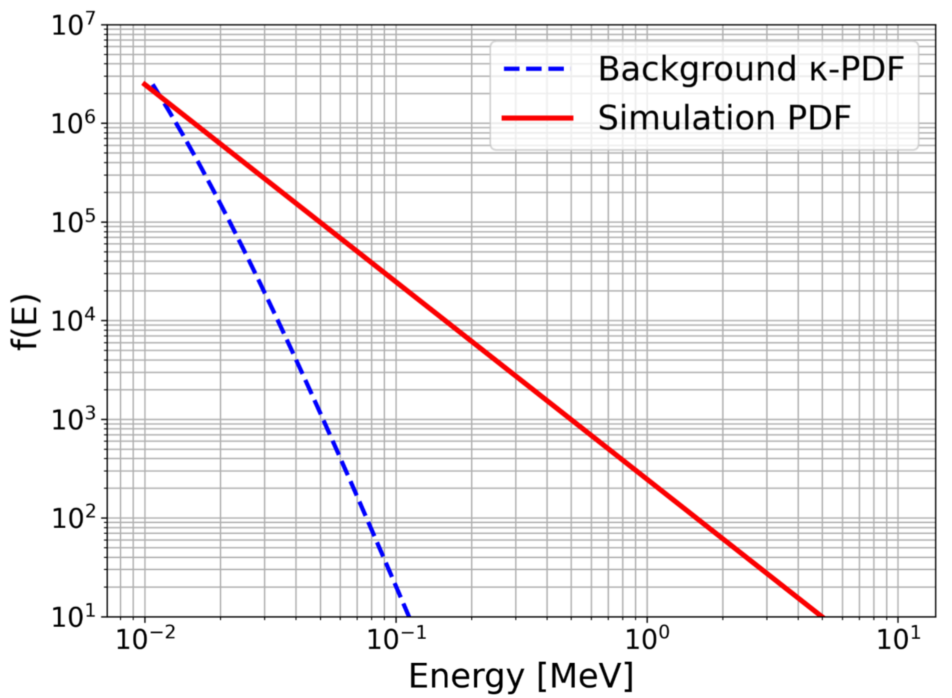

Husidic et al. (submitted)

Intensity Curves

- Roll-over:
  - 165 – 300 MHz for ζ = 30
  - 65 – 145 MHz for ζ = 70
- Lower roll-over frequencies observed at side/top views
- Spectral shapes not yet power-law, but already steeper than analytical predictions

$\alpha = (\delta - 1)/2$ $\alpha = 0.9\,\delta - 1.22$

- Strong self-absorption and evolving distributions steepen spectra early on
- Idealised synchrotron/GS models miss key complexities in evolving CME environments
- Observations often show steeper indices → trend consistent with our particle transport simulations

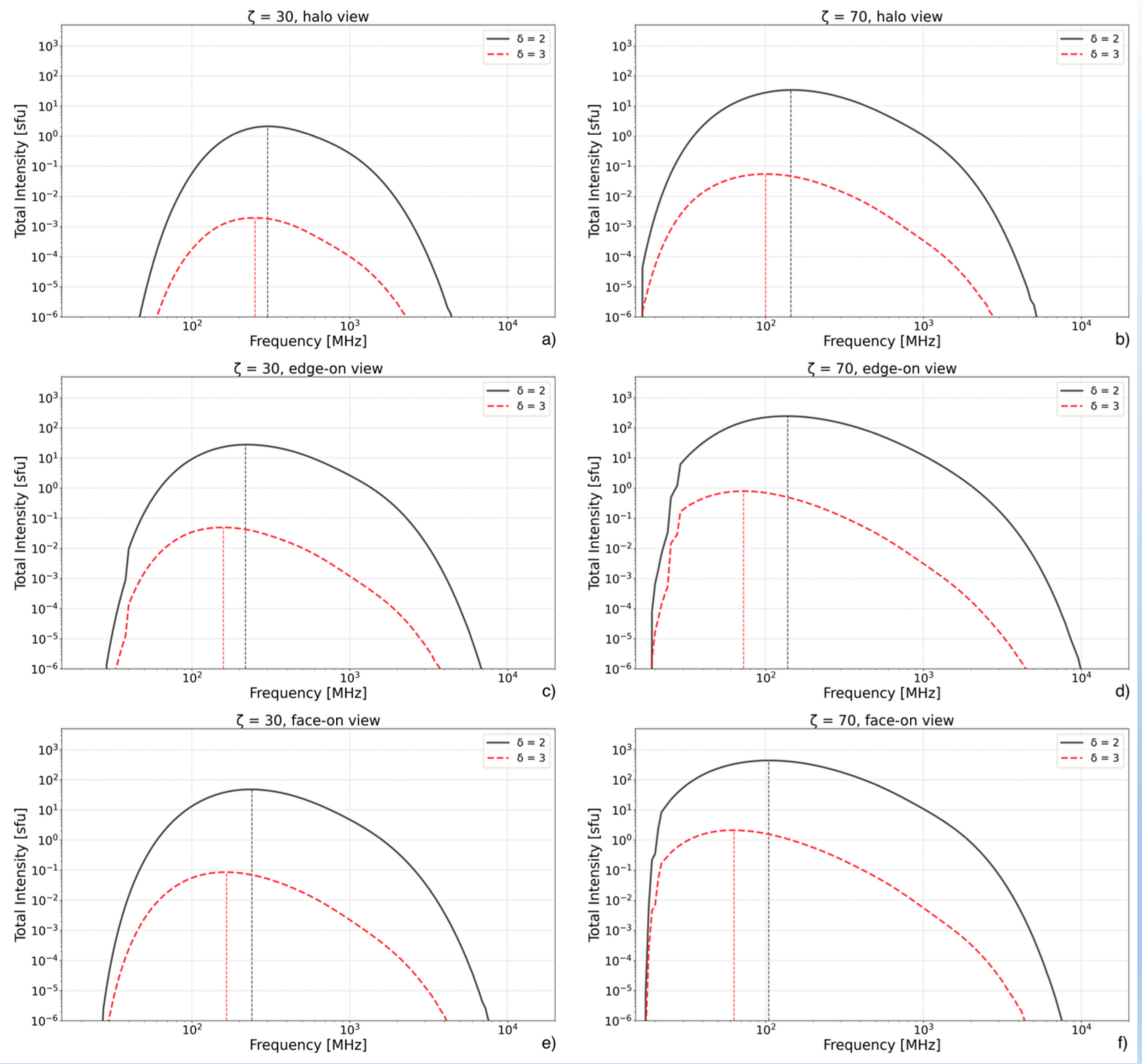

Husidic et al. (submitted)

Weighted Magnetic Field Strength

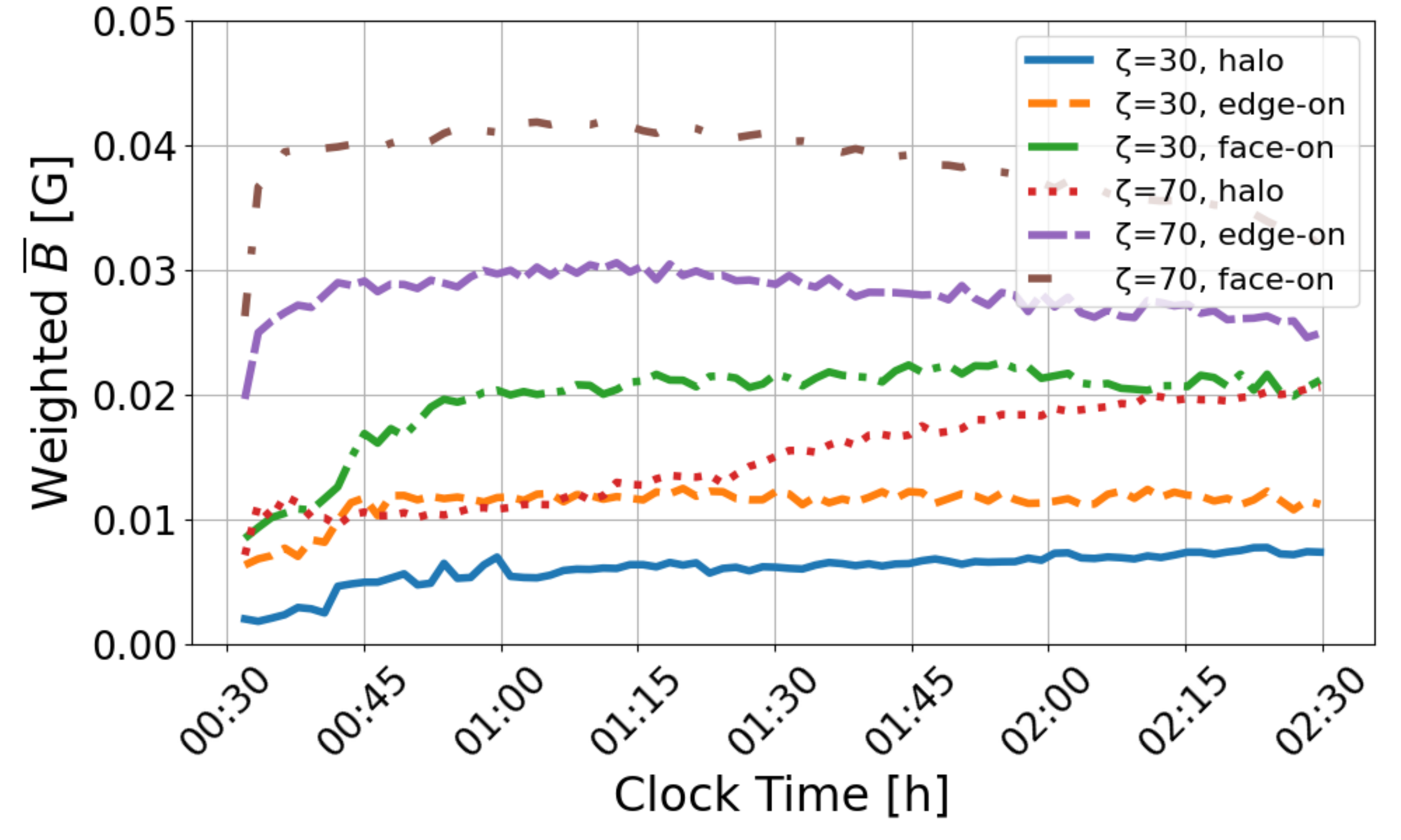

Husidic et al. (submitted)

Itô Calculus

$$\frac{\partial f}{\partial t} + \frac{d\mathbf{x}}{dt} \cdot \nabla f + \frac{d\mu}{dt}\frac{\partial f}{\partial \mu} + \frac{dp}{dt}\frac{\partial f}{\partial p} = \frac{\partial}{\partial \mu}\left(D_{\mu\mu}\frac{\partial f}{\partial \mu}\right) + \nabla \cdot (\mathbf{D}_{\perp} \cdot \nabla f)$$

- The FTE is **equivalent** to the **stochastic differential equations (SDEs)**:

$$\begin{aligned} d\mathbf{x} &= \left(\frac{d\mathbf{x}}{dt} + \nabla \cdot \mathbf{D}_{\perp}\right) dt + \sqrt{2\mathbf{D}_{\perp}}\, d\mathbf{w}_{\mathbf{x}}, \\ d\mu &= \left(\frac{d\mu}{dt} + \frac{\partial D_{\mu\mu}}{\partial \mu}\right) dt + \sqrt{2D_{\mu\mu}}\, dw_{\mu}, \\ dp &= \frac{dp}{dt} dt, \end{aligned}$$

  with $\boldsymbol{w_i}$ being Wiener processes (= Brownian motion)

- SDEs describe the trajectory of a **pseudo-particle** in phase space

- Pseudo-particle ≈ phase space density element

Itô Calculus

- **PARADISE** solves the FTE by integrating the equivalent SDEs forward in time, i.e.,

$$
\left.
\begin{aligned}
d\mathbf{x} &= \left(\frac{d\mathbf{x}}{dt} + \nabla \cdot \mathbf{D}_\perp\right) dt + \sqrt{2\mathbf{D}_\perp}\, d\mathbf{w}_\mathbf{x},\\
d\mu &= \left(\frac{d\mu}{dt} + \frac{\partial D_{\mu\mu}}{\partial \mu}\right) dt + \sqrt{2D_{\mu\mu}}\, dw_\mu,\\
dp &= \frac{dp}{dt} dt,
\end{aligned}
\right\}
$$

Integrate and sample ~10^8 pseudo-particles

- The average solar wind velocity and magnetic field are obtained from the 3D ideal MHD models **EUHFORIA** or **Icarus**

- The diffusion coefficient are derived from a composite slab/2D turbulence model with the assumptions of QLT or a non-linear theory (modular)

Cross-Field Diffusion Coefficients

- Axis-symmetric cross-field diffusion tensor: $\mathbf{D}_\perp = D_\perp \left(\mathbb{I} - \mathbf{bb} \right)$
- Perpendicular mean free path: $\lambda_\perp = \frac{3}{v} \kappa_\perp = \frac{3}{2v} \int_{-1}^{+1} \mathrm{d}\mu \; D_\perp(\mu)$
- Different assumptions about the turbulence give different diffusion coefficients
- Implemented in PARADISE (modular):
  1. Non-linear guiding center theory
     $$\lambda_\perp = \left[3^{(q+1)/2} D(s,q) \frac{\delta B_{2D}^2}{B_0^2} l_{2D}^{q+1} \right]^{2/(q+3)} \left[\Gamma\left(\frac{1+q}{2}\right) \Gamma\left(\frac{1-q}{2}\right) \right]^{2/(q+3)} \lambda_\parallel^{(1-q)/(3+q)}$$
  2. Field line random walk: $\lambda_\perp = \sqrt{\frac{3(s-1)}{2(q-1)}} l_{2D} \frac{\delta B_{2D}}{B_0}$
  3. Empirical models:
     1. Dröge et al. (2010): $\lambda_\perp = \alpha \lambda_\| r_g$ wit $r_g = \frac{\sqrt{1-\mu^2} p}{|q| B}$
     2. Zhang et al. (2009): $\lambda_\perp = \lambda_\perp^0 \left(\frac{p}{p_{\mathrm{ref}}} \right)^{b_1} \left(\frac{B_{\mathrm{ref}}}{B} \right)^{b_2}$
  4. $\lambda_\perp = \text{constant}$